J Mater Sci (2011) 46:2991–2997
DOI 10.1007/s10853-010-5176-y

Characterization of hot extruded Mg/SiC nanocomposites fabricated by casting

Hongseok Choi · Noé Alba-Baena · Sunya Nimityongskul · Milton Jones · Tom Wood · Mahi Sahoo · Roderic Lakes · Sindo Kou · Xiaochun Li

Received: 8 September 2010 / Accepted: 8 December 2010 / Published online: 6 January 2011
© Springer Science+Business Media, LLC 2011

Abstract Mg–1%SiC nanocomposites were fabricated using an ultrasonic cavitation based casting method, resulting in the dispersion of the reinforcing SiC nanoparticles to form Mg–metal matrix nanocomposite (Mg–MMNC) billets. The MMNC billets were then processed using hot extrusion at 350 °C. Micrographic observations illustrate a significant grain size reduction and the presence of microbands that align the SiC nanoparticles parallel to the direction of extrusion for Mg–MMNCs. Observations from the cross-section at 90° of the extrusion direction show uniform nanoparticles dispersion. Results from the extruded Mg–MMNCs tensile testing at different temperatures (25, 125 and 177 °C) reveal an increase of the yield strength, ultimate tensile strength, and ductility values as compared to the un-reinforced and extruded Mg-alloy; such increase was also observed from the microhardness testing results where an increase from 19 to 34% was measured.

H. Choi · N. Alba-Baena · S. Nimityongskul · X. Li (✉)
Department of Mechanical Engineering, University of Wisconsin-Madison, Madison, WI 53706, USA
e-mail: xcli@engr.wisc.edu

M. Jones
Materials Science Program, University of Wisconsin-Madison, Madison, WI 53706, USA

T. Wood
GS Engineering, Inc (GSE), Houghton, MI 49931, USA

M. Sahoo
CANMET Materials Technology Laboratory, Ottawa, ON K1A 0G1, Canada

R. Lakes
Department of Engineering Physics, University of Wisconsin-Madison, Madison, WI 53706, USA

S. Kou
Department of Materials Science and Engineering, University of Wisconsin-Madison, Madison, WI 53706, USA

Introduction

Magnesium alloys are becoming ever more prevalent in electronics, automotive, and aerospace industries as energy conservation and performance demands increase. Mg alloys are one-third lighter than the equal volume of aluminum alloys, and this fact is one of the contributing factors that makes these alloys so desirable [1, 2]. Production of goods using Mg alloys has been mostly in the field of pressure die casting because of its high productivity and dimensional accuracy [3]. Extrusion is very useful for its technical and economic advantages in the production of structural components. Magnesium alloys offer high specific strength, superior damping capability, excellent machinability, and good electromagnetic shielding characteristics [3]. However, Mg alloys exhibit poor mechanical performance at elevated temperatures [1, 2], their applications are usually limited to temperatures below 120 °C; in consequence, the improvement in the high-temperature mechanical properties of magnesium alloys will expand their industrial applications [4]. In general, the use of thermally stable ceramic reinforcements to create Mg based metal matrix composites (MMC) facilitates the retention of enhanced mechanical properties at elevated temperatures [4]. The desirable characteristics of MMCs include enhancements in stiffness, strength, creep resistance, and wear resistance [5]; however, MMCs normally provide lower ductility than the original matrix [4]. Cao et al. [6, 7] have reported that nanocomposites can increase the ductility of as-cast magnesium-based metal matrix

nanocomposites (MMNCs). Furthermore, by using silicon carbide (SiC) nanoparticles, Cao et al. [6–12] (among others) have reported enhancement in yield strength and tensile strength without the loss of ductility by reinforcing the matrix with small volumes (<2%) of ceramic nanoparticles. However, the production of magnesium-based metal matrix nanocomposites (MMNCs) is extremely challenging by conventional casting and mechanical stirring methods. Such methods have not been successful in fabricating MMNCs due (among others) to the high specific surface area of nanoparticles and the poor wettability between nanoparticles and molten metal [8]. On the other hand, the use of a technique that combined solidification processes with ultrasonic cavitation based dispersion of nanoparticles in metal melts achieved promising results for a uniform dispersion and distribution of reinforcing nanoparticles in Mg–MMNCs [6–12]. During this process, ultrasonic cavitations generate micro "hot spots" with temperatures of approximately 5000 °C, pressures exceeding 1000 atm, and heating rates exceeding 10^{10} K/s [13]. During MMNCs processing once nanoparticles are added to the melt, any air bubbles trapped around nanoparticle agglomerates serve as nucleation sites for cavitation generating the desired nanoparticle dispersion [9]. Such process requires that the nanoparticle agglomerations stay in the cavitation zone enough time so it can be achieved a more efficient dispersion.

This paper shows results in implementing the ultrasonic cavitation based casting process using a cage enclosure for isolate such cavitation zone. The niobium cage was used to keep the nanoparticles inside the molten metal and under ultrasonic cavitation zone as efficient as possible, while the molten metal was still allowed to flow in and out of the cage with holes. This ultrasonic process was used to fabricate pure Mg and Mg–1%SiC nanocomposite billets for hot extrusion. After extrusion, the mechanical properties of the MMNC rods were tensile tested at 25, 125, and 177 °C. Finally, to observe the dispersion of nanoparticles and grain sizes in extruded MMNCs, optical micrographs, and SEM images were obtained using samples from the tensile specimens.

Experimental procedure

Figure 1 illustrates the experimental setup schematic of ultrasonic cavitation based solidification processing of SiC nanoparticles (average 50 nm from NanoAmor) in an Mg matrix (99.93% pure from USMagnesium). The experimental system was comprised of resistance heating furnace for melting the magnesium alloy, nanoparticle feeding mechanism, protective gas system, and an ultrasonic processing unit. The crucible used for melting and ultrasonic

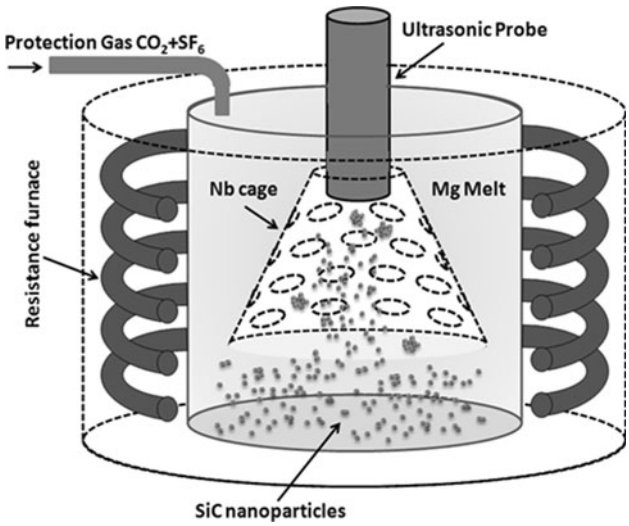

Fig. 1 Schematic of experimental setup for fabricating nanocomposites

processing was made of mild steel with an inside diameter of 114 mm and a height of 127 mm. A Permendur power ultrasonic probe made of niobium C-103 alloy was used to generate a 17.5 kHz and maximum 4.0 kW power output (Advanced Sonics, LLC, Oxford, CT) for melt processing. The niobium C-103 probe is 31.12 mm in diameter and 223.5 mm in length. The ultrasonic probe was dipped into the melt about 13 mm. A thin walled niobium cage (31.8 mm upper diameter, 88.9 mm base diameter; 76.2 mm high, 254 μm wall thickness) in a shape of truncated cone was used to hold nanoparticles inside the melt pool during the ultrasonic processing. The niobium cage has a total of 55 holes 7.94 mm in diameter to allow the circulation of the melt and nanoparticles. 800 g of Mg was melted in the steel crucible while being protected by CO_2 and 0.75% SF_6. Once the melt temperature of 700 °C was attained the niobium cage containing 1 wt% β-SiC nanoparticles was submerged in the melt beneath the ultrasonic probe. The average size of the SiC nanoparticles used was 50 nm. The melt was then ultrasonically processed at 3.5 kW power level for 15 min for the samples with and without SiC nanoparticles. The ultrasonic probe and niobium cage were then removed from the melt and the melt was elevated to a pouring temperature of 725 °C. The melt was cast into a steel permanent mold purged with CO_2 + 0.75% SF_6 and preheated to 350 °C, which was designed and fabricated to produce a cast billet of 63.5 mm in diameter and 102 mm in length. The casting was allowed to cool for 30 min before the mold was opened and the billet was removed. A graphite pouring cup was used to guide the melt into the mold, and also mounts a Pyrotech SIVEX ceramic foam filter (55 × 55 × 12 mm, 20 pores/in).

The cast billets were preheated for 2 h prior to extrusion, and were extruded at 350 °C to obtain rods of 12.7 mm in diameter. The rods were extruded at a 25:1 ratio, with a ram speed of 10 mm/s and a load of 500 tons. The extruded rods of 12.7 mm in diameter were then machined into tensile bars of approximately 105 mm long with a 35 mm gauge length and 6.0 mm diameter. Tensile specimens were tested at 25, 125, and 177 °C. The tensile specimens were tested in an Instru-Met TTC 90 in (228.6 cm) 4,535.92 kg load frame using an Epsilon 3542-0100-050-HT2 extensometer with a 25.4 mm gage length clamped to each specimen. The furnace and tensile grips were preheated to the test temperature. The test specimens were then loaded into the tensile grips and the furnace was re-heated to testing temperature. The specimens were held at the testing temperature for 10 min before testing to ensure a uniform temperature distribution. The cross-head velocity was set to 1.27 mm/min and the test was run until the specimen failure. The specimens were removed from the furnace and test fixture within 30 s and allowed to air cool to room temperature. The microstructures of the tested samples were studied by optical microscopy and scanning electron microscopy (SEM). Samples were cut, mounted, and manually ground and polished from the grip sections of the tensile bars after tensile testing. The extruded samples were then etched with 5% acetic acid in 95% water for 30 s. Average grain size was measured using the linear intercept method from optical micrographs of the samples taken at room temperature. SEM imaging was conducted using a LEO 1530 machine. Microhardness tests were conducted with a Buehler Micromet 2003 microhardness tester (load 500 gf, load time 30 s). Finally, microhardness tests were conducted at room temperature from specimens that had undergone tensile testing.

Experimental results

Mechanical properties

The average yield strength, tensile strength, and ductility for the Mg and Mg–1%SiC tensile specimens conducted at various temperatures are shown in Fig. 2. At room temperature and with the addition of 1%SiC to the Mg, there are significant enhancements in yield strength by 49% (from 93 to 133 MPa), tensile strength increases from 198 to 224 MPa (+13%), and ductility raise by 37% (from 5.9 to 8.1%). Below recrystallization temperature for Mg and at 125 °C there are moderate enhancements in yield strength (by 18%, 65 MPa for pure Mg and 77 MPa for Mg–1%SiC) and tensile strength (by 15%).

However, a significant increase in ductility (by 85% measuring 13.8% for pure Mg and 25.4% for the Mg–1%SiC nanocomposite) with the addition of 1%SiC. Also shown in Fig. 2, at 177 °C and after the recrystallization temperature of Mg (150 °C [14, 15]), there is almost no enhancement in yield strength (by only 3%, 55 MPa for pure Mg and 57 MPa for Mg–1%SiC), a moderate enhancement in tensile strength and 11% only (from 88 to 97 MPa), while a significant increase in ductility was averaged (91%) with the addition of 1%SiC (20.9 and 39.9%, respectively). In future, to further evaluate the Mg–1%SiC high-temperature performance a creep test should be completed to compare the extruded pure Mg and

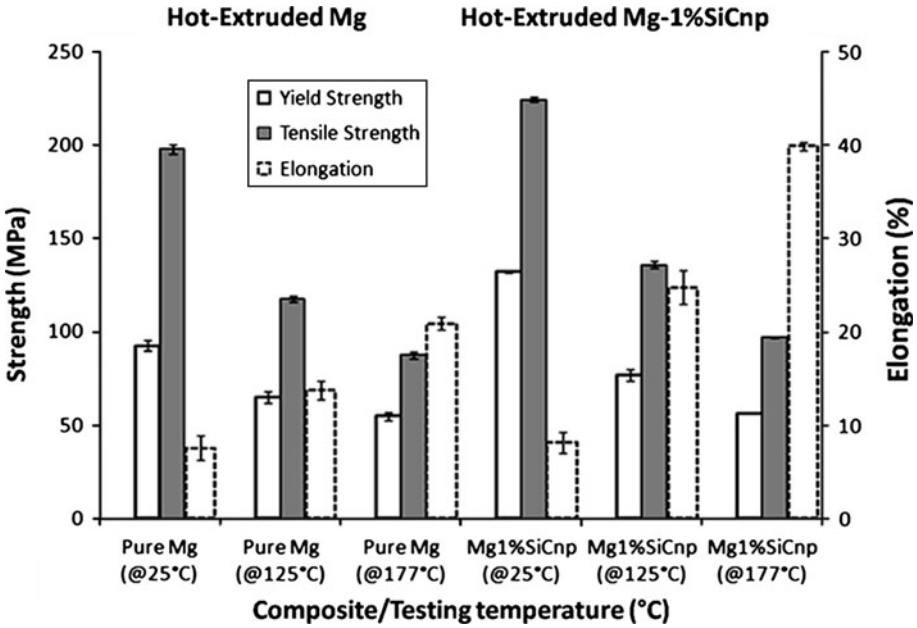

Fig. 2 Tested properties of hot extruded pure Mg and Mg–1%SiC at 25, 125, and 177 °C

Mg–1%SiC samples. The consistent increase in ductility with the addition of 1%SiC nanoparticles is in contrast to the ductility decrease that was previously reported with the addition of microparticles and fibers to Mg matrix [7]. Results show that the addition of 1%SiC nanoparticles was able to enhance yield strength, tensile strength, and ductility indicating that a thermally stable bond exists between the reinforcing particles and the matrix, for the temperatures tested: lower and after recrystallization temperatures. The significantly enhanced ductility at 125 and 177 °C with the addition of 1%SiC is mainly attributed to the uniform dispersion (see Figs. 4, 5a) of thermally stable nanoparticles throughout the matrix. Based in the characterization done by Cao et al. [7]; the Mg/SiC interface behavior showing no intermediate phases at the interface of Mg and SiC, and found that the SiC nanoparticles were well bonded to the matrix. Then, SiC nanoparticles aid in maintaining the grain structure in the extruded Mg–1%SiC by pinning grain boundaries at elevated temperatures thus resulting in higher ductility.

Table 1 shows the average microhardness of the specimens tested at room temperature, 125, and 177 °C, respectively. Microhardness of 125 and 177 °C specimens were taken after mechanical testing and conducted at room temperature. At room temperature the average microhardness of Mg and Mg–1%SiC was 29.2 and 39.0 HV, at 125 °C the averages were 30.8 and 39.3 HV and at 177 °C were 31.6 and 37.7. The microhardness enhancements of extruded Mg–1%SiC compared to extruded Mg at 25, 125, and 177 °C are 34, 28, and 19%, respectively. The performance increases in microhardness at all temperatures is largely attributed to the reinforcement that SiC nanoparticles to the Mg matrix.

Characterization

Table 1 also shows average grain size longitudinal to the direction of extrusion in the specimens tested at 25, 125, and 177 °C. Samples were examined finding the average grain size longitudinal to the direction of extrusion for extruded Mg and extruded Mg–1%SiC are consistent and slightly smaller for the different MMNCs at the different temperatures (33, 30 and 7%, respectively). In general the average grain size was measured in 33 and 25 μm, but is observing a large grain size variation, respectively, for the pure Mg and the MMNC. There is not significant grain refinement between the Mg and Mg–1%SiC due to dynamic recrystallization (DRX) during hot extrusion at 350 °C. Grains begin to recrystallize at initial grain boundaries in hot extrusion growing in layers until the old grains are consumed as described by Buschow et al. [16] and reported by Liu et al. [17]. DRX is thought to initiate at original (prior to extrusion) grain boundaries due to an accumulation of dislocations at the grain boundaries during the hot extrusion [17].

Table 1 Average microhardness and grain sizes of the hot extruded Mg and Mg–1%SiC samples

Temperature (°C)	Microhardness (HV)		Grain size (average, μm)	
	Pure Mg	Mg–1%SiC	Pure Mg	Mg–1%SiC
25	29.2 ± 1.1	39 ± 2.1	33 ± 11	22 ± 4
125	30.8 ± 1.4	39.3 ± 0.8	36 ± 27	25 ± 12
177	31.6 ± 1.5	37.7 ± 0.4	30 ± 7	28 ± 7

Optical micrographs are representative images in the longitudinal (extruded) direction of extruded Mg and extruded Mg–1%SiC tested at 25, 125, and 177 °C, are shown in Fig. 3. The SiC bands in Figs. 3b, 2d, and f show SiC nanoparticle micro-sized agglomerations. Such agglomerations are not the only regions that SiC are located in; however, larger concentrations and clusters of SiC nanoparticles form these bands. The most distinguishing characteristic between the extruded Mg samples (see Fig. 3a, c, e) and the extruded Mg–1%SiC (Fig. 3b, d, f) are the dark SiC bands running parallel to the axis of extrusion, while the grain structures keep similar in each pair of images (compare Fig. 3a and b, c and d or e and f). Wang et al. [18] observed similar phenomena in pure Mg with 40 μm sized SiC particles after extruded at a ratio of 13:1. Streaks of SiC microparticles were observed parallel to the direction of extrusion; however, there were no clusters of SiC microparticles and the particles were bonded well to the matrix. Similar bands have also been observed in extruded Mg alloys with intermetallics that have been destroyed and dispersed into bands during the extrusion process (see Fig. 4 in Liu et al. [17]).

As observed in Fig. 3b, d, and e the alignment is much more accentuated in the composites extruded at high-temperature (Fig. 3e), than in the composites extruded at low temperature (Fig. 3b). Figure 4 shows a sequence of SEM images that illustrates the SiC nanoparticle bands along the extrusion direction. The representative images from an Mg–1%SiCnp nanocomposite tested at room temperature (25 °C) shows also the micro-banded structure and free zones which is typical in this type of materials (Fig. 4b). Detailed view of a micro-band (in Fig. 4c) shows the SiC nanoparticle distribution following the micro-bands' path, however, preserving its dispersion.

Analyzing an area of SEM image in Fig. 4a, energy dispersive X-ray spectroscopy (EDS) images confirms that the microbands observed in Fig. 3b, d, and f are in fact SiC nanoparticles (see Fig. 5). EDS spectral imaging in Fig. 5d shows the SiC nanoparticle bands in an Mg matrix in the longitudinal direction, while in contrast Mg spectral

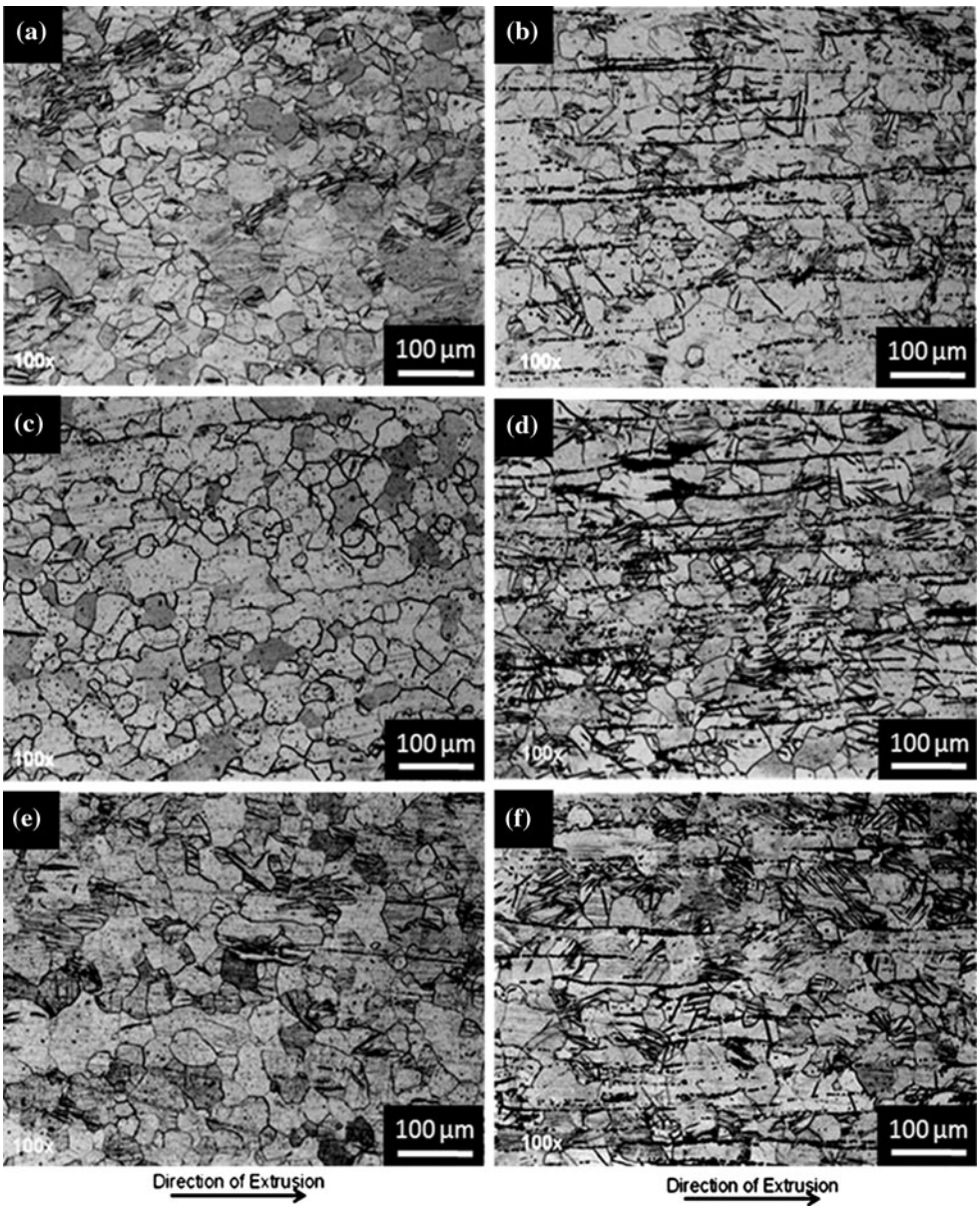

Fig. 3 Optical micrographs in longitudinal (extruded) direction of extruded specimens: **a** Mg tested at 25 °C, **b** Mg–1%SiC tested at 25 °C, **c** Mg tested at 125 °C, **d** Mg–1%SiC tested at 125 °C, **e** Mg tested at 177 °C, **f** Mg–1%SiC tested at 177 °C

(Fig. 5c) image shows its complement. Image in Fig. 6a shows an as-cast sample transverse direction to the extrusion.

Figure 6 show the homogenous distribution of the SiC nanoparticles. Agglomerations are dispersed across the sample while nanoparticles are present also along the sample as seen in Fig. 6b. This confirms that even though clusters of nanoparticles exist in the composite samples, tensile tests revealed that the SiC nanoparticles increased the ductility at all temperatures tested. One of the primary reasons for the increase in ductility is the bonding that exists between the SiC nanoparticles and Mg, besides the reduction of voids in clusters of nanoparticles.

Conclusions

Ultrasonic cavitation based solidification processing achieves a uniform dispersion and distribution of reinforcing SiC nanoparticles in the Mg matrices. After extrusion process and particle migration the distribution remains observable in the transverse direction. SiC nanoparticles were well dispersed in the cross-section transverse to the direction of extrusion. While in the longitudinal direction the nanoparticles arrange along the extrusion direction but remaining dispersed. The extruded MMNC billets contained microbands of SiC nanoparticles oriented parallel to the direction of extrusion. Micrographs show no

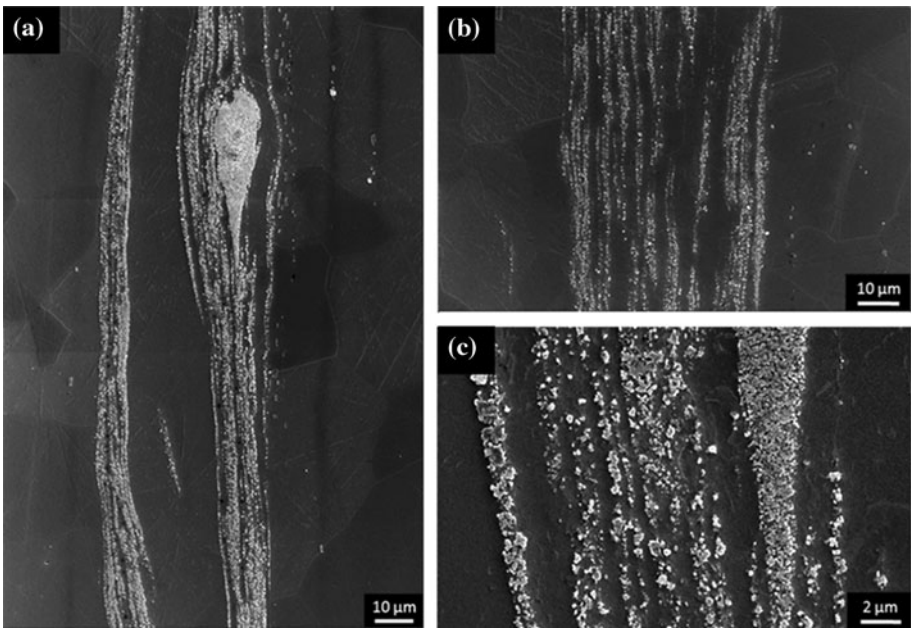

Fig. 4 SEM image sequence of an Mg–1%SiCnp nanocomposite sample tested at 25 °C. **a** Composed image of a micro-banded structure, **b** detail of the free zones accompanying the microbands, and **c** view of SiC nanoparticles distributed in the microbands

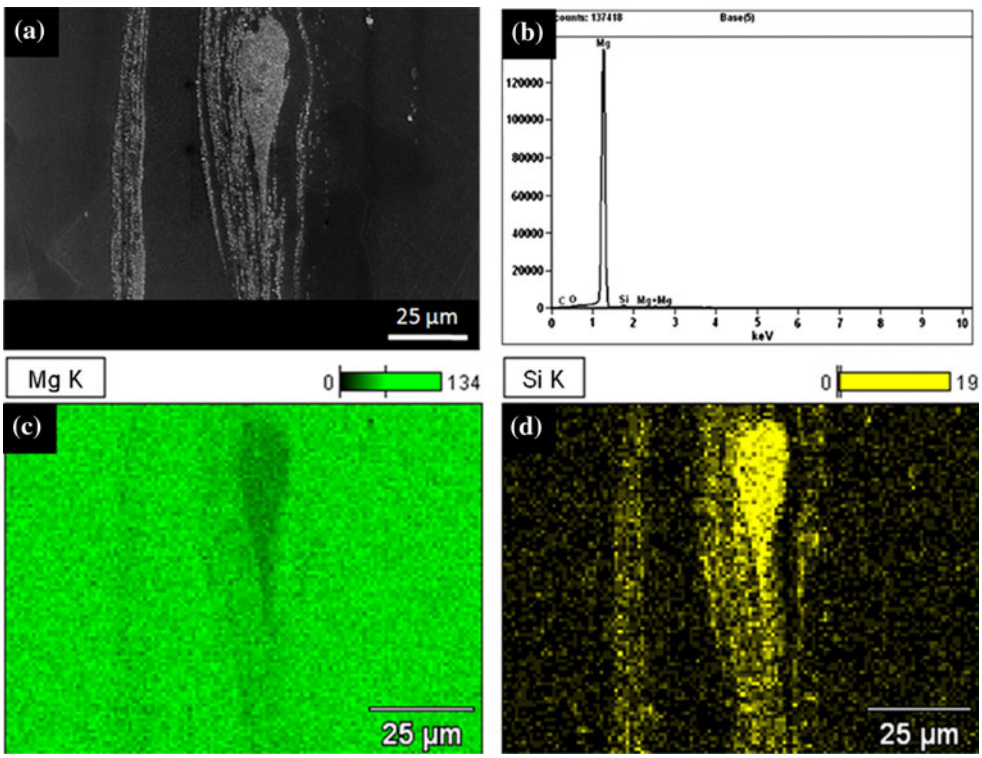

Fig. 5 **a** SEM image of a micro-band area, **b** EDS of Mg–1%SiC 177 °C, **c** Mg K, and **d** Si K at longitudinal (extruded) direction

significant grain refinement between the Mg and Mg–1%SiC MMNC samples after hot extrusion. However, the addition of 1%SiC nanoparticles consistently increases the ductility and enhances other mechanical properties. Yield strength, tensile strength and microhardness were improved also as compared to the extruded Mg samples at various temperatures. Comparing these results to previous reports, that shows with the addition of microparticles and fibers to Mg matrix the ductility decreases for various temperature conditions, the use of SiC nanoparticles, in contrast, enhance the ductility of the Mg composite for such temperature conditions.

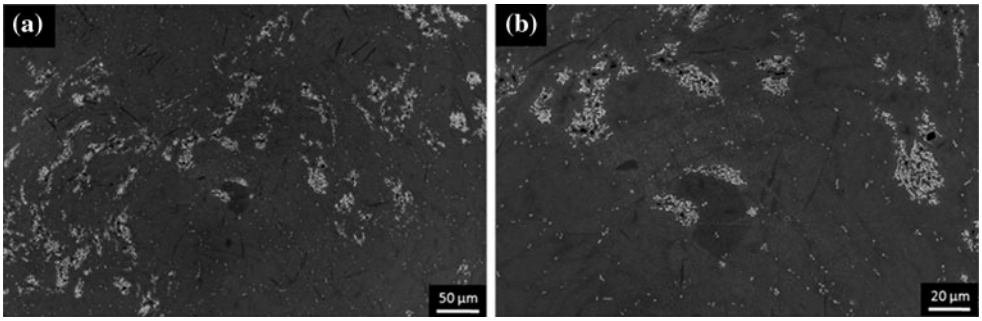

Fig. 6 **a** SEM image in transverse (extruded) direction of the SiC nanoparticle and **b** a closer view of the SiC nanoparticle agglomerations dispersion in a Mg–1%SiCnp sample after tested at room temperature

Acknowledgements This work was supported by National Science Foundation and American Foundry Society. The authors thank US Magnesium for its donation of Mg ingots.

References

1. Friedrich H, Mordike B (2006) In: Magnesium technology—metallurgy, design data, applications. Springer–Verlag, Berlin, p 219
2. Czerwinski F (2007) Magnesium injection molding. Springer, New York, p 1
3. Chen Y, Wang Q, Peng J, Zhai C, Ding W (2007) J Mater Process Technol 182:281
4. Ye H, Liu X (2004) J Mater Sci 39:6153. doi:10.1023/B:JMSC.0000043583.47148.31
5. Clyne T, Withers P (1993) An introduction to metal matrix composites. Cambridge University Press, Cambridge, p 454
6. Cao G, Konishi H, Li X (2008) J Manuf Sci Eng 130:31105-1
7. Cao G, Choi H, Konishi H, Kou S, Lakes R, Li X (2008) J Mater Sci 43:5521. doi:10.1007/s10853-008-2785-9
8. Lan J, Yang Y, Li X (2004) Mater Sci Eng A 386(1–2):284
9. Cao G, Kobliska J, Konishi H, Li X (2008) Metall Mater Trans A 39(4):880
10. Li X, Duan Z, Cao G, Roure A (2007) Trans Am Foundry Soc 115:747
11. Cao G, Konishi H, Li X (2008) Mater Sci Eng A 486(1–2):357
12. Yang Y, Lan J, Li X (2004) Mater Sci Eng A 380:378
13. Suslick K, Didenko Y, Fang M, Hyeon T, Kolbeck K, McNamara W, Mdleleni M, Wong M (1999) Philos Trans R Soc Lond A 357:335
14. Chalmers JB (1962) Physical metallurgy. Wiley, New York
15. Davis JR (1998) Metals handbook. ASM International, New York
16. Buschow K, Cahn R, Flemings M, Ilschner B, Kramer E, Mahajan S (2008) Encyclopedia of materials: science and technology. Elsevier, Amsterdam, p 2375
17. Liu K, Zhang J, Rokhlin L, Elkin F, Tang D, Meng J (2009) Mater Sci Eng A 505:13
18. Wang R, Song Y, You S, Surappa M (2000) Microstructure and interface structure of SiC-reinforced Mg metal matrix composite. In Aghion E, Eliezer D (eds) Proceedings of the 2nd Israeli international conference on magnesium science and technology 2000. Magnesium 2000, Israel, Magnesium Research Institute, p 229